Hindawi Publishing Corporation
Science and Technology of Nuclear Installations
Volume 2012, Article ID 375070, 18 pages
doi:10.1155/2012/375070

Research Article

Major Achievements and Prospect of the ATLAS Integral Effect Tests

Ki-Yong Choi, Yeon-Sik Kim, Chul-Hwa Song, and Won-Pil Baek

Korea Atomic Energy Research Institute, Daedeok-daero 989-111, Yuseong-Gu, Daejeon 305-353, Republic of Korea

Correspondence should be addressed to Ki-Yong Choi, kychoi@kaeri.re.kr

Received 15 August 2011; Accepted 12 November 2011

Academic Editor: Klaus Umminger

A large-scale thermal-hydraulic integral effect test facility, ATLAS (Advanced Thermal-hydraulic Test Loop for Accident Simulation), has been operated by KAERI. The reference plant of ATLAS is the APR1400 (Advanced Power Reactor, 1400 MWe). Since 2007, an extensive series of experimental works were successfully carried out, including large break loss of coolant accident tests, small break loss of coolant accident tests at various break locations, steam generator tube rupture tests, feed line break tests, and steam line break tests. These tests contributed toward an understanding of the unique thermal-hydraulic behavior, resolving the safety-related concerns and providing validation data for evaluation of the safety analysis codes and methodology for the advanced pressurized water reactor, APR1400. Major discoveries and lessons found in the past integral effect tests are summarized in this paper. As the demand for integral effect tests is on the rise due to the active national nuclear R&D program in Korea, the future prospects of the application of the ATLAS facility are also discussed.

1. Introduction

ATLAS (Advanced Thermal-Hydraulic Test Loop for Accident Simulation) is a large-scale integral effect test facility with a reference plant of APR1400 (Advanced Power Reactor, 1400 MWe), which is under construction in Korea [1]. It was designed to have the capability of simulating various transients and accident conditions at full pressure and temperature conditions, including loss of coolant accident (LOCA) series as well as non-LOCA series. The ATLAS program started in 1997 under a nuclear R&D program funded by the Korean government. The complete installation of ATLAS was finished in 2005. In 2006, extensive commissioning operations were carried out, including startup tests and preliminary tests [2].

In 2007, ATLAS was used for a wide range of integral effect tests on the reflood phase of a large break LOCA to resolve the safety issues of the APR1400 raised by a regulatory body [3]. Afterwards, at the beginning of 2008, ATLAS was modified to have a configuration for simulating the direct vessel injection (DVI) line break accidents of the APR1400. One of the unique design features of ATLAS is its ability to simulate the DVI of the emergency core cooling water. Sensitivity tests for different DVI line break sizes were performed and an integral effect database was established for various break sizes of 5%, 25%, 50%, and 100% [4].

After a series of DVI line break tests were completed, small break LOCA (SBLOCA) tests commenced at the end of 2008. In order to provide an integral effect database for SBLOCA of the APR1400, sensitivity tests for different break sizes of the cold leg have been conducted. In addition, parameter survey tests were also taken into account in a test matrix in order to investigate the effects of break location. In addition, a counterpart test to the 6-inch SBLOCA data of the Large-Scale Test Facility (LSTF) in Japan was performed in order to evaluate the scaling of the ATLAS facility.

Among the DVI line break scenarios, 50% of the cross-section of a DVI nozzle was of interest because this break size is on the edge of the criterion provided by the EPRI requirement, where a core uncovery should be prevented by a best-estimate methodology [5]. In particular, the thermal-hydraulic phenomena occurring in the upper annulus downcomer region between the DVI nozzle and the cold leg nozzles are expected to be complicated due to the countercurrent flow of the upward break flow and the downward safety injection flow. Thus, the 50% DVI line break database was

selected as the 50th International Standard Problem (ISP-50) sponsored by the OECD/NEA Committee on the Safety on Nuclear Installation (CSNI) Working Group on Analysis and Management of Accidents (WGAMA) in 2009. The ISP-50 was started with a blind calculation, followed by an open calculation. It was successfully finished by approval of CSNI in 2011 [6].

The steam generator tube rupture (SGTR) events were investigated from the year 2010. A single-tube rupture and five-tube rupture events were successfully simulated in the ATLAS facility. The effects of leakage from either the hot side or cold side were examined for sensitivity work.

When the major integral effect tests on LOCA series accidents were completed, typical non-LOCA events were conducted from the second half of the year 2010, including the feed line break (FLB) and steam line break (SLB). Tests were performed either in conservative or in best-estimated initial and boundary conditions to support the nuclear industry and validate the safety analysis codes, respectively.

2. Scaling Methodology of the ATLAS

The three-level scaling methodology which consists of integral scaling, boundary flow scaling, and local phenomena scaling proposed by Ishii et al. [7] was applied to the design of ATLAS. There have been plenty of discussions concerning the height scaling, and finally the 1/2 height scaling was chosen based on the following key rationales [1]. (a) There is no absolute superiority between full- and half-height designs, and a decision should be made by considering the test objectives, prototype design characteristics, budget, and so on. (b) The integrated annular downcomer, which can be realized more easily in the half-height design, is superior to an externally separated downcomer in simulating multi-dimensional phenomena in a reactor vessel downcomer and in revealing new phenomena. (c) In the case of a direct vessel injection, the thermal-hydraulic phenomena expected to occur in the upper downcomer of the reactor vessel need further physical understanding. (d) There is no Integral Effect Test (IET) data for an Reactor Coolant System (RCS) with a DVI as in the APR1400; test data for the LBLOCA reflood and DVI line break will be valuable for a phenomena understanding and code assessment. (e) Air-water visualization tests reveal that there is no significant difference in the flow patterns for downcomer gaps of over around 2.5 cm [8]. (f) A lower height than 1/2 would induce too high a surface heat flux and many difficulties during the installation stage. Finally, the 1/2-height, 1/144-area scaling was selected by considering the available downcomer gap size, flow velocity, and nozzle distance [8].

After the integral scaling ratio was determined, in the second scaling level a boundary flow scaling methodology was applied, especially to the design of the break nozzle, containment, and relief valves. Mass inventory and energy balance was carefully taken into account to minimize scaling distortion during integral effect tests. For instance, several sets of spool pieces were fabricated depending on the test scenarios.

Table 1: Scaling table of the ATLAS facility.

Parameters	Scaling law	ATLAS design
Length	l_{OR}	1/2
Diameter	d_{OR}	1/12
Area	$d^2{}_{OR}$	1/144
Volume	$l_{OR}d^2{}_{OR}$	1/288
Velocity	$l^{1/2}{}_{OR}$	$1/\sqrt{2}$
Time	$l^{1/2}{}_{OR}$	$1/\sqrt{2}$
Flow rate	$l^{1/2}_{OR}d^2{}_{OR}$	1/203.6
Core ΔT	ΔT_{OR}	1
Core power	$l^{1/2}{}_{OR}d^2{}_{OR}$	1/203.6
Heat flux	$1/l^{1/2}{}_{OR}$	$\sqrt{2}$
Power/volume	$1/l^{1/2}{}_{OR}$	$\sqrt{2}$
Pressure drop	l_{OR}	1/2
Pump head	l_{OR}	1/2
Core rod diameter	1	1
SG U-tube diameter	$l^{1/2}{}_{OR}$	$1/\sqrt{2}$
No. of core rods	$d^2{}_{OR}$	1/144
No. of SG U-tubes	N_{OR}	1/72
SG U-tube heat transfer area	$l_{OR}l^{1/2}{}_{OR}N_{OR}$	1/203.6

In the third scaling level, local important phenomena which should be preserved in a scaled facility were examined, and the design was optimized to preserve those phenomena. In the primary piping, a flow pattern and a flow regime transition are the key phenomena, and the Froude number governs such phenomena. Thus, the horizontal sections of the primary piping were optimized to preserve the Froude number in ATLAS. Important local phenomena to be considered in a pressurizer are the critical flow of the surge line for LBLOCA, the critical flow of the safety valves, the CCFL in the surge line, and the offtake at the hot leg-to-surge line. Specially designed sleeves that can be easily installed and removed were manufactured and can be used depending on the test of interest. Void fraction and flow regime transition are the key local phenomena to be preserved in a reactor pressure vessel (RPV) downcomer gap, especially when boiling occurs. Finally, the downcomer gap size was slightly increased from 21 mm to 26.2 mm to preserve the effects of flow regime. The increased downcomer volume was counterbalanced by decreasing the same amount of volume in the lower plenum of the reactor pressure vessel. The major phenomena of concern in the steam generator are CCFL in the U-tubes and forward/reverse heat transfer. The internal tube diameter can be determined either by preserving the Wallis number, or heat transfer area. Here, the Wallis number of each phase j_k^* is defined as the follows:

$$j_k^* = \frac{j_k}{\sqrt{gD\left(\rho_f - \rho_g\right)/\rho_k}}, \tag{1}$$

where j_k^* and ρ_k are the superficial velocities and densities of phase k ($k = g$ for gas phase and $k = f$ for liquid phase), D is the tube diameter, and g the gravitational acceleration. In ATLAS, the U-tube diameter was determined by preserving the heat transfer area. A summarized scaling table of the ATLAS facility is shown in Table 1.

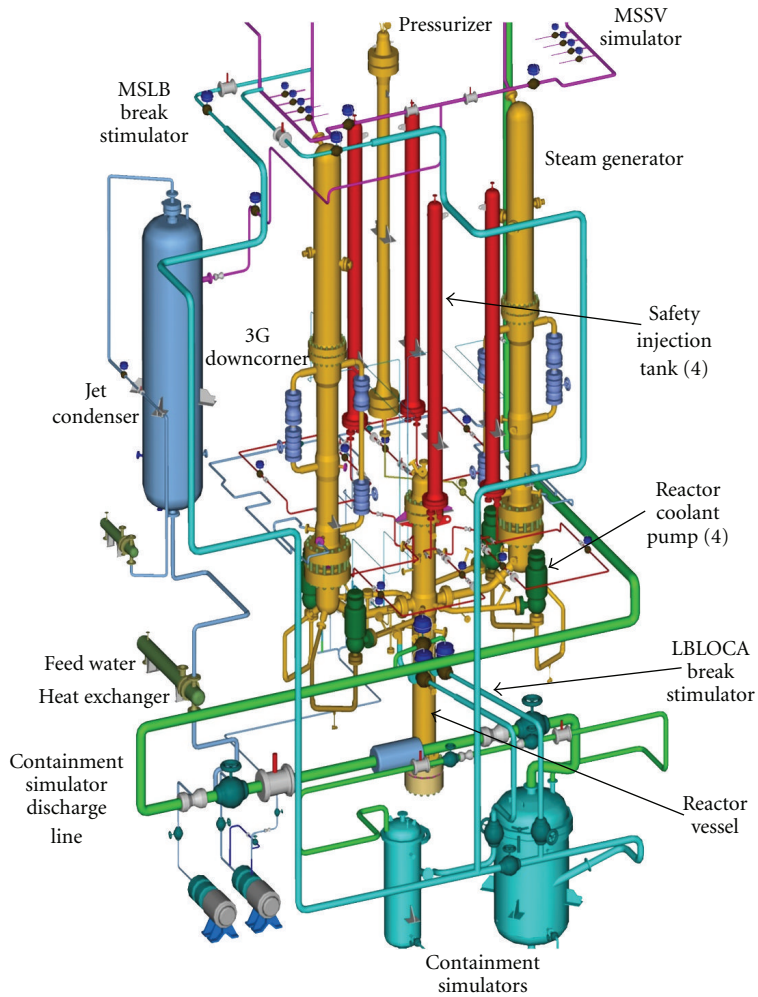

Figure 1: Schematic arrangement of the major components of ATLAS.

3. Major Design Features

ATLAS was designed to operate under prototypic pressure and temperature conditions. Its design pressure and temperature is 18.7 MPa and 370°C, respectively. Water is used as the working fluid, and thus property similarity between APR1400 and ATLAS is achieved. All equipment was made in stainless steel to avoid corrosion. It consists of a primary system, secondary system, safety system, auxiliary system, power supply system, instrumentation and control system, and data acquisition system (DAS). The same geometrical loop configuration as the APR1400 was maintained from a scaling viewpoint. All crucial components were designed and fabricated according to the ASME B&PV, Section-VIII, and Division 1 or 2 code. The core consists of 396 electrically heated rod, and the maximum power is 2.0 MW, which is around 10% of the scaled core power. It was heavily instrumented and the total number of measurement channels is over 1250. A schematic arrangement of the major components is shown in Figure 1. Further detailed information on the design features of ATLAS can be found in the literature [1, 2].

Compared with other major large-scale facilities that were built and operated in the past, ATLAS is a half-height facility. ATLAS was added to the existing sketch by Aksan [9] and compared with other facilities as shown in Figure 2. It can be seen from the sketch that ATLAS is a unique facility with 2 hot legs and 4 cold legs. Though ATLAS is a half-height facility, the inner diameter of the reactor pressure vessel is comparable to those of other facilities. In particular, the aspect ratio (l/d) of ATLAS has a similar value to that of the LSTF. Above all, ATLAS is equipped with four DVI nozzles for Emergency Core Cooling (ECC) injections, which is one of the special design features.

4. Major Outcomes of the Previous IETs

Since the complete installation of the ATLAS facility in 2005, a series of integral effect tests have been performed, with priority given to major design basis accidents. Major outcomes from the previous ATLAS tests relevant to nuclear safety are summarized in the following subsections.

4.1. LBLOCA Reflood Tests. The test for the LBLOCA reflood phase was selected as the first test item of the ATLAS facility,

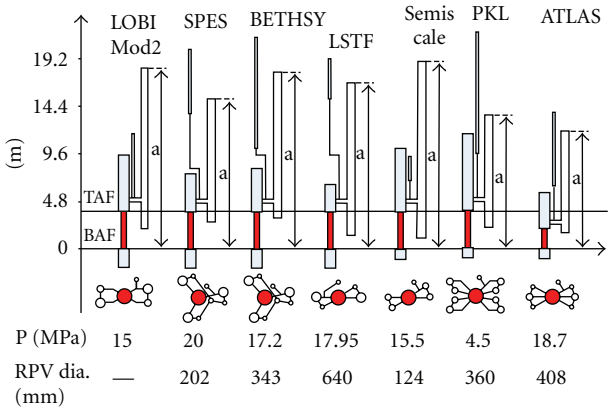

Figure 2: Comparison of ATLAS with the other facilities.

as a few safety concerns were raised regarding the thermal-hydraulic safety performance of the emergency core cooling system during LBLOCAs in the licensing review for the APR1400's Standard Design Approval: (a) the overall validity of the safety analysis code and analysis methodology for the reflood phase of LBLOCAs, regarding the direct ECC bypass, and (b) the adverse effect of downcomer boiling during the late reflood phase of large-break LOCAs.

These two phenomena are expected to occur in the annular downcomer region during a LBLOCA. These issues were raised due to a new safety feature of a DVI system that supplies the ECC directly into the reactor vessel downcomer. Unlike the conventional cold leg injection system, it has become important to quantify the ECC bypass at the upper downcomer along the lateral direction to the break during the reflood phase. Figure 3 schematically depicts the ECC bypass mechanism in the DVI system during the reflood phase. It is generally known that there are two ECC bypass mechanisms, a sweepout and a direct ECC bypass. A sweepout is caused by the steam injected from the intact cold legs, which interacts with the coolant in the downcomer and causes the coolant to be discharged to the broken cold leg. From the UPTF test results [10], it was found that a direct ECC bypass is the major bypass mechanism of the DVI system. The ECC bypass has been identified as playing an important role in the depletion of the coolant inventory in the reflood phase of an LBLOCA.

Therefore, an extensive series of tests were conducted to provide reliable integral and separate effect test data for resolution of the above issues. The ATLAS reflood test program progressed into two serial phases (Phase 1 and Phase 2) according to the target period to be simulated. The main objective of the Phase 1 tests was to identify the major thermal-hydraulic characteristics during the late reflood phase of a LBLOCA, and its main concern was the parametric effects on downcomer boiling [11]. The Phase 2 test was subsequently continued. The main objective of the Phase 2 tests was to investigate the thermal-hydraulic characteristics during an entire reflood period to provide reliable data to help validate the LBLOCA analysis methodology for the APR1400. Among the whole test matrix of the LBLOCA reflood tests, LB-CL-09, LB-CL-11, LB-CL-14, and LB-CL-15 were seriously analyzed to support the licensing process of the APR1400 in Korea, and their results dealing with the experimental results and analysis were already published [12–15]; only the major outcomes are summarized in this paper. Key test matrix for the LBLOCA tests is shown in Table 2.

In phase 1, LB-CL-05 was analyzed to investigate the effects of the downcomer boiling and safety injection flow rate. Figure 4 compares the measured collapsed water levels in the core and downcomer with those by the MARS code [16], which indicates deeper depressions in the water levels than the data. The maximum surface temperature variation of the core heater rods is shown in Figure 5. The MARS code predicted a much higher rod temperature than the data. In the MARS simulation, the peak rod temperature reached up to 792°C, possibly by an insufficient ECC injection due to the downcomer boiling in the downcomer region. In the test, however, the downcomer boiling was identified but the peak rod temperature was as low as 284°C. Based on these comparison results, it can be concluded that the downcomer boiling is a real phenomenon occurring in the lower downcomer regions, as expected in the safety analysis code, but its effects were not as significant as the code prediction. It was found that the interfacial drag model in the MARS code is responsible for the collapsed water level so the model needs to be carefully investigated by the code developers.

In phase 2, both the conservative initial and boundary condition (LB-CL-09) and best-estimate conditions (LB-CL-11, LB-CL-14) were simulated. A separate effect test at a much lower reflooding velocity condition (LB-CL-15) was supplemented in the test matrix to validate the RELAP5 reflood models for a core quenching phenomenon under a low flow rate ECC injection condition.

The maximum heater rod surface temperature during the LB-CL-09 test is shown in Figure 6. In this test, the reflooding was controlled to start at 1912 s [13]. The heater surface temperatures were measured at 12 axial locations, and the maximum surface temperature of the heater rod was 722°C. A temperature increase by 257°C from the reflood start time was obtained. A top quenching phenomenon was also observed in every heater group, but the quenching did not show radial homogeneity. The core heaters were quenched

Table 2: Key test matrix for the LBLOCA reflood tests.

Test ID	Test conditions
LB-CL-05	Separate effect test (Phase-1) (i) Late reflood condition focusing on downcomer boiling effect
LB-CL-09	Integral effect test at conservative condition (i) Decay power: ANS73x120% (ii) Containment pressure: 0.1 MPa (iii) Power distribution: radially uniform
LB-CL-11	Integral effect test at BE condition (i) Decay power: ANS79x102% (ii) Containment pressure: 0.2 MPa (iii) Power distribution: radially uniform
LB-CL-14	Integral effect test at BE condition (i) Decay power: ANS79x102% (ii) Containment pressure: varying (iii) Power distribution: radially non-uniform
LB-CL-15	Separate effect test (i) Complementary test at low reflooding rate

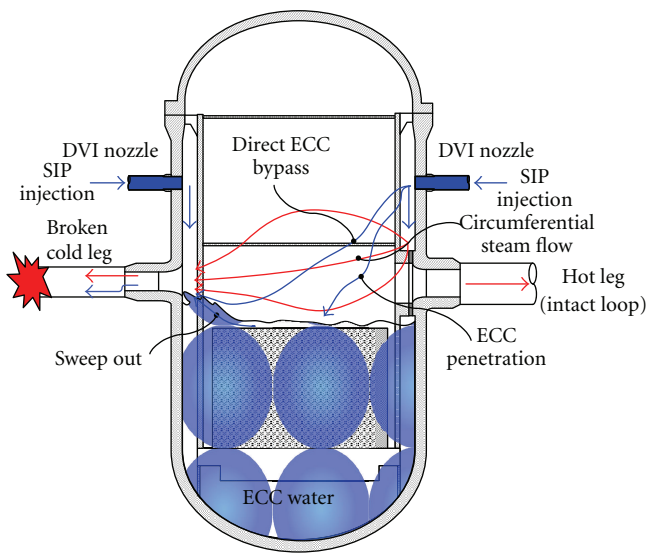

Figure 3: A schematic diagram of the direct ECC bypass and sweepout phenomena.

in the order of the middle region, center region, and outer region.

Figure 7 shows a typical ECC bypass ratio obtained from the LB-CL-11 test [14]. The ECC bypass ratio is defined as follows:

$$R_{\mathrm{ECC,bypass}} = \frac{W_{\mathrm{ECC,bypass}}}{W_{\mathrm{ECC}}} = \frac{W_{\mathrm{break,water}}}{W_{\mathrm{ECC}}}, \quad (2)$$

where $W_{\mathrm{ECC,bypass}}$, $W_{\mathrm{break,water}}$, and W_{ECC} are the bypassed ECC flow rate, the water component of a break flow, and the injected ECC flow rate. The obtained ECC bypass fraction shows a great fluctuation ranging from 0.2 to 2.1, especially during the initial period. Such great fluctuation turned out to be due to the sweepout occurring significantly during the earlier period. The ECC bypass rate was between 0.2 and 0.6 during the later period except for some irregular peaks. A similar trend in the ECC bypass ratio was found in the other tests.

A comprehensive integral effect database regarding the LBLOCA reflood phase of the APR1400 was successfully established through the above-mentioned LBLOCA program. Details of the test conditions were chosen based on in-depth discussions held occasionally with a regulatory organization and nuclear industries for a straightforward application of the test results toward the urgent licensing process of the APR1400. Korean industries used the LB-CL-15 data to obtain licensing approval from a regulatory organization and have been performing further detailed calculations by utilizing LB-CL-09, LB-CL-11, and LB-CL-14 in order to develop or improve their own safety analysis methodology of an LBLOCA.

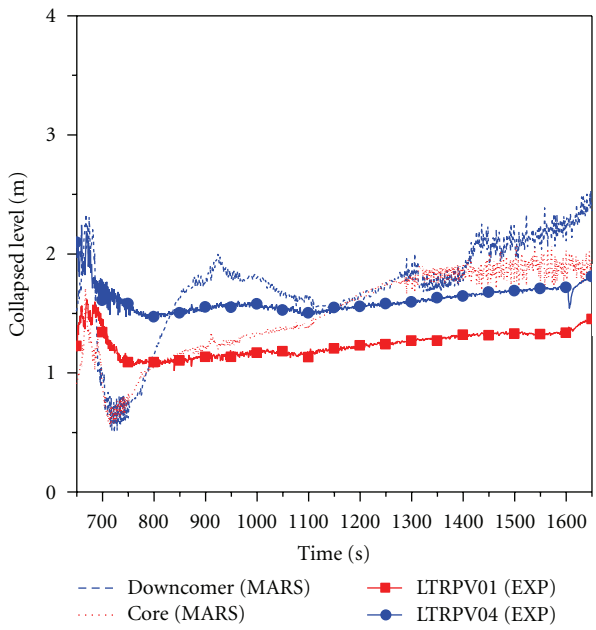

Figure 4: Comparison of measured water levels in the core and the downcomer with code calculations during LB-CL-05.

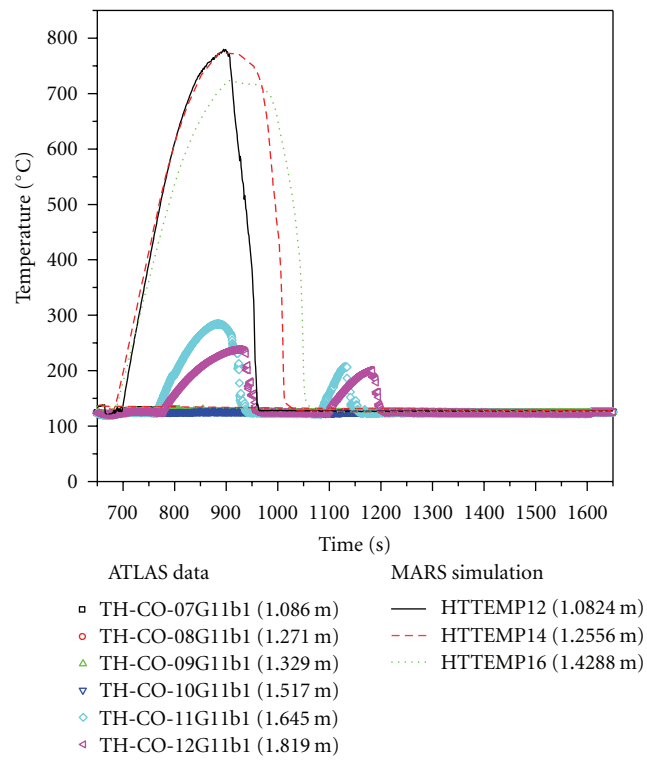

Figure 5: Comparison of measured PCTs with code predictions during LB-CL-05.

4.2. DVI Line SBLOCA Tests. A direct vessel injection (DVI) concept was first proposed in the Utility Requirement Document (URD) by the Electric Power Research Institute (EPRI) in the early 1990s. The AP600 (or the AP1000) was the first reactor to adopt a DVI method for an emergency core cooling system instead of a conventional cold leg injection method. The double-ended severance of a DVI line is taken as a limiting break case for a SB-LOCA analysis of the AP1000. The US-APWR also selected the DVI method for delivering borated ECC water from safety injection pumps into the core. The VVER-1000 passively injects borated water by four pressurized accumulation tanks into the reactor core through separate inlet nozzles attached to the reactor pressure vessel. In Korea, the APR1400 adopted the DVI method as one of the improved safety features compared with the OPR1000.

Those DVI-adopted plants treat a DVI line break as another spectrum among the SBLOCAs in their safety analysis because a DVI nozzle directly attached to a reactor vessel is vulnerable to a postulated break from a safety viewpoint. The thermal hydraulic phenomena in the RPV downcomer are expected to be different from those in the cold leg injection mode during postulated design basis accidents. In the event of a DVI line break, the vapor generated in the core is introduced to the RPV downcomer through the hot legs, steam generators, and cold legs. The vapor should then pass through the upper part of the RPV downcomer to be discharged through the broken DVI nozzle. Thus, a complex flow pattern and multi-dimensional aspects are anticipated, especially in the upper downcomer region. Thus, DVI relevant data and a reliable prediction tool for a DVI line break scenario are required by both regulators and industry.

Thus far, sensitivity tests on the break size were performed to establish an integral effect database for various break sizes: 5%, 25%, 50%, and 100% [3, 4, 17]. A test matrix for the DVI line SBLOCA tests is shown in Table 3.

Table 3: Test matrix for the DVI line SBLOCA tests.

Test ID	Break size APR1400 (%/inch)	Break size Break nozzle dia. (mm)	Remarks
SB-DVI-03	100%/8.5	15.13	Double-ended break
SB-DVI-04	25%/4.25	7.63	
SB-DVI-05	25%/4.25	7.63	Repeat of SB-DVI-04
SB-DVI-06	5%/1.9	3.41	
SB-DVI-07	50%/6.0	10.8	
SB-DVI-08	100%/8.5	15.13	Repeat of SB-DVI-03
SB-DVI-09	50%/6.0	10.8	ISP-50 test

All tests were performed with an assumption of loss of off-site power simultaneously with the break, and the worst single failure as a loss of a diesel generator, resulting in a minimum safety injection flow to the core. Furthermore, the safety injection flow to the broken DVI-4 nozzle was not credited. Eventually, ECC water was injected from one safety injection pump located opposite the broken DVI nozzle and three safety injection tanks, as shown in Figure 8.

Figure 9 shows the effects of the break size on the primary pressure; code prediction results by the MARS code are also plotted for comparison. In each break case, a clear pressure plateau was observed just before the loop seal clearing.

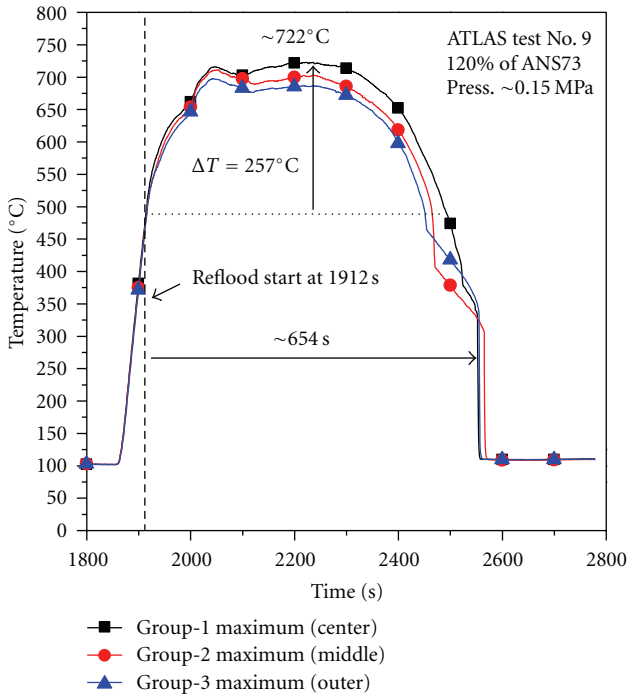

Figure 6: Maximum heater rod surface temperature variation of the core during LB-CL-09.

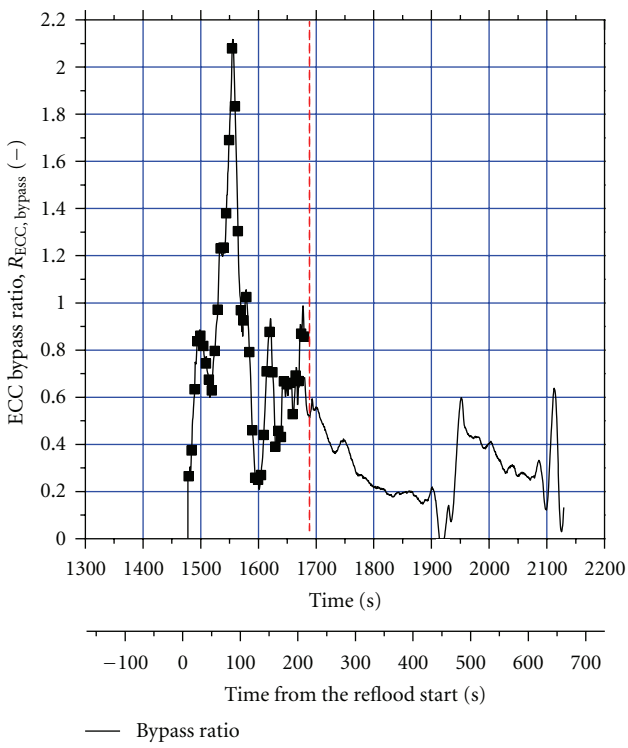

Figure 7: Comparison of estimated ECC bypass ratio with code calculations during LB-CL-11.

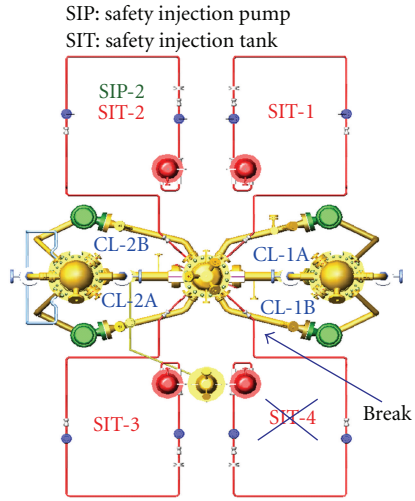

Figure 8: A loop arrangement for a DVI line break with a single failure assumption.

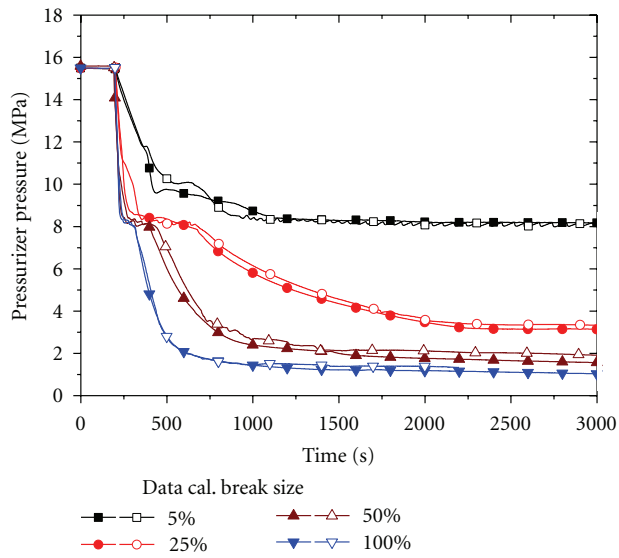

Figure 9: Effects of the break size of the DVI nozzle on the primary pressure.

As the break size became larger, the plateau became milder and lasted shorter.

Comparisons of the collapsed water levels of the core and downcomer with the calculated levels for a typical 100% break case are shown in Figure 10. In cases of breaks larger than 50%, the core was observed to be partly uncovered, leading to increases in the PCT. Such initial core level decreases were recovered when the loop seals in the intermediate legs were cleared. Thus, it was experimentally confirmed that the loop seal clearing plays a critical role in determining the minimum water level in the core, and consequently the PCT.

Among the test series, the 50% break case was selected for the 50th international standard problem (ISP-50) of the OECD/NEA in 2009. The ISP-50 consisted of two serial phases: blind and open phases. Sixteen calculations were

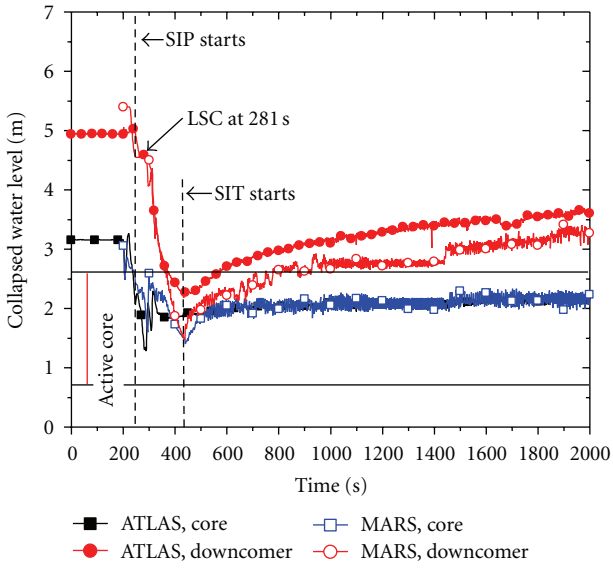

Figure 10: Comparison of collapsed core and downcomer water levels for a 100% DVI line break.

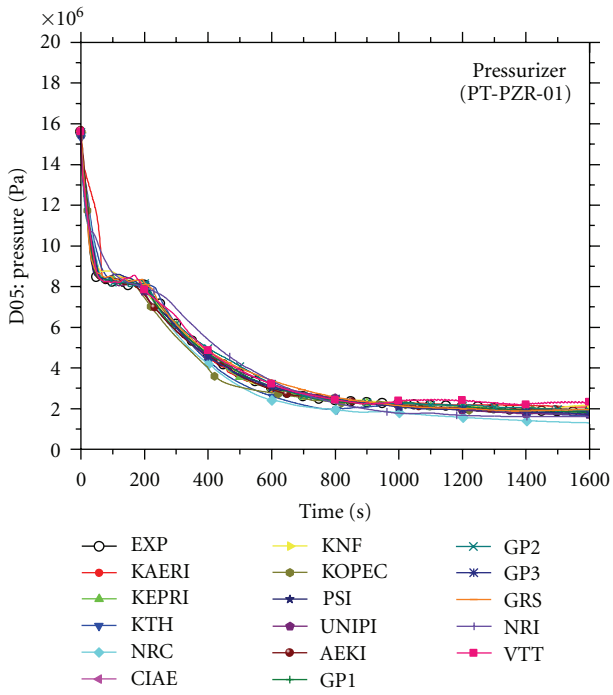

Figure 11: Comparison of the calculated primary pressures with the measurement (SB-DVI-09).

collected from 11 OECD countries, and seven leading safety analysis codes were utilized: RELAP5 series, MARS, TRACE 5.0, CATHARE, ATHLET, APROS, and KORSAR/GP. Detailed information on ISP-50 can be found in the final integration report [6]. Typical comparison results of the primary pressure and break flow rate are shown in Figures 11 and 12, respectively.

In this ISP-50 exercise, multidimensional phenomena such as ECC mixing in the upper downcomer observed in the

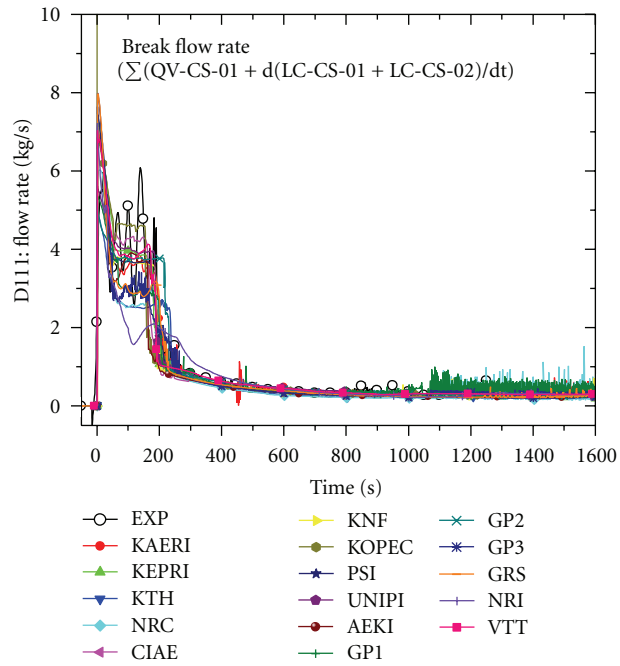

Figure 12: Comparison of the calculated break flow rates with the measurement (SB-DVI-09).

test were highlighted in terms of code prediction capability. In particular, detailed calculation results on the downcomer fluid temperatures were requested and compared. In the test, the cold ECC water introduced through the DVI nozzles was well mixed with the hot water in the upper downcomer region. However, such vigorous and instant mixing was not predicted appropriately by most codes. The fluid temperature of the intact loop side annulus was much lower than that of the broken side annulus. Temperature stratification in an azimuthal direction was predicted even in a lower downcomer region. A typical comparison of the downcomer fluid temperature in the upper downcomer region with the measurement is shown in Figure 13. The detailed downcomer fluid temperature measurement locations are shown in Figure 14. Six thermocouples were installed at six different elevations.

Another multidimensional aspect observed in the DVI line break test was a nonuniform distribution of the PCT; the PCT increased earlier in the side core region than in the center core region. In order to investigate this nonuniformity, a 3D calculation was performed with the MARS-3D and the TRACE code during the ISP-50 exercise. Figure 15 shows a typical mass flux distribution in the core region. The center region where the mass flux is high was effectively cooled, whereas the side region where the mass flux is either relatively low or negative was not adequately cooled, resulting in an increase in the PCT.

4.3. Cold Leg SBLOCA Tests. Many integral effect tests on cold leg SBLOCAs have been performed since the Three Mile Island Unit 2 accident. Either the existing facilities were modified or new facilities were built to perform SBLOCA

Table 4: Test matrix for the cold leg SBLOCA tests.

Test ID	Break size APR1400 (%/inch)	SI injection	Remark
SB-CL-01	1.78%/4	SIP-1, 3 and 4 SITs	
SB-CL-02	4.0%/6	SIP-1, 3 and 4 SITs	Closed core bypass path
SB-CL-03	7.11%/8	SIP-1, 3 and 4 SITs	
SB-CL-04	8.03%/8.5	SIP-1, 3 and 4 SITs	
SB-CL-05	1.78%/4	SIP-1, 3 and 4 SITs	Repeat of SB-CL-01
SB-CL-06	4.0%/6	SIP-2 and SIT-1, 2, 3	CPT for SB-DVI-09
SB-CL-07	0.44%/2	SIP-1, 3 and 4 SITs	No loop seal
SB-POSRV-01	2 POSRV/3.5	SIP-1, 3	IOPOSRV
SB-POSRV-02	1 POSRV/2.3	SIP-1, 3	IOPOSRV
SB-CL-08	4.0%/6	SIP-1, 3 and 4 SITs	Cold leg injection
SB-CL-09	4.0%/6	SIP-1, 3 and 4 SITs	
SB-CL-10	5.0% (LSTF)	4 SITs (CLI)	CPT for LSTF SB-CL-18 test

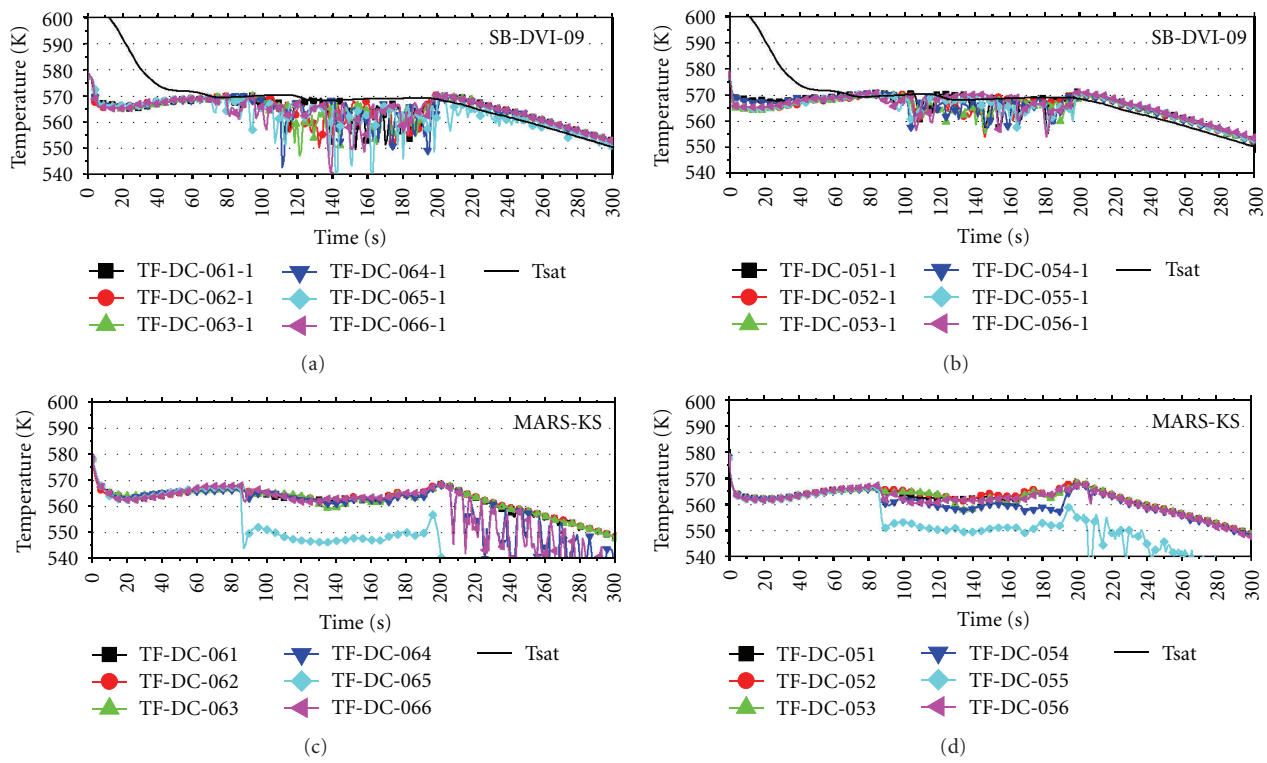

Figure 13: Comparison of upper downcomer fluid temperature with the measurement (SB-DVI-09).

tests. As the APR1400 has a unique loop configuration compared with the conventional nuclear power plants, two loops with two hot legs and four cold legs, there is a practical limit to apply the existing IET database to validate the safety analysis codes for the APR1400. Furthermore, the APR1400 was designed to inject ECC water not through the cold leg nozzle but through the DVI nozzles in the case of SBLOCAs. Thus, the DVI performance needs to be reevaluated and compared with the cold leg injection method. No integral effect database for DVI injection during SBLOCAs has yet been reported.

In order to establish a wide database for a cold leg SBLOCA, a test matrix was determined as shown in Table 4. First, the effects of break size from equivalent diameters of 2 to 8 inches of the APR1400 were investigated. All breaks were directed downward from the bottom side of the cold leg. Similar to the DVI break case, the assumption of loss of offsite power simultaneously with the break, resulting in the minimum safety injection flow to the core, was used. Then, two safety injection pumps and four safety injection tanks are available to provide ECC water into the core. In addition, several parametric effects were experimentally investigated:

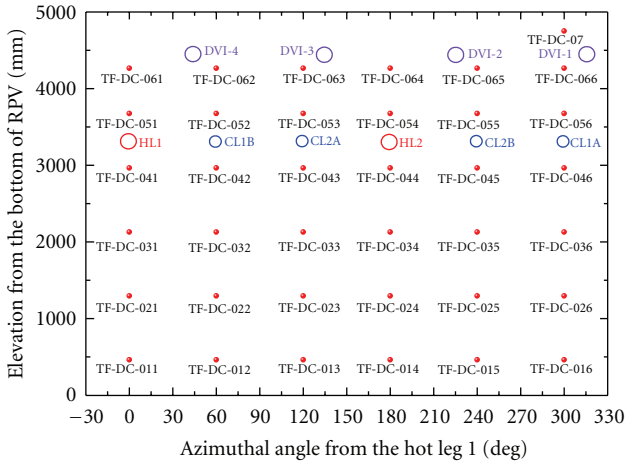

Figure 14: Measurement locations for downcomer fluid temperatures.

the effects of RPV bypass flow (SB-CL-02 versus SB-CL-09), effects of ECC injection (SB-CL-08 versus SB-CL-09), and counterpart test to the DVI line break (SB-CL-06 versus SB-DVI-09). Inadvertent opening of the pilot operated safety valve (IOPOSRV) with two different break sizes were also simulated in ATLAS. Finally, a counterpart to the SB-CL-18 test, which was performed using a large-scale test facility (LSTF) by JAEA, was accomplished. The scalability of ATLAS to real nuclear power plants was investigated using this counterpart test.

Five typical phases characterizing a SBLOCA scenario were identified in the test, as shown in Figure 16: (1) blow-down, (2) natural circulation, (3) loop seal clearance, (4) boil-off, and (5) core recovery [18, 19]. The duration of each phase depends on the break size and performance of the ECCS. Characteristic parameters such as the primary pressure (PT-PZR-01), secondary pressure (PT-SGSD1-01), and collapsed water level of the downcomer (LT-RPV-04A) were also plotted for comparison.

The blow-down phase is characterized by a rapid depressurization of the primary system until a flashing of the reactor coolant starts, and by an increase in the secondary pressure up to the opening of the main steam-safety valves (MSSVs). The break flow is maintained in a single-phase liquid during the blow-down period. The next phase is characterized by a two-phase natural circulation before the loop seal formation. A loop seal clearance and boil-off phase then follow. Finally, the core recovery phase starts when the ECC water is injected by the safety injection tank.

Effects of the break location were experimentally investigated by performing two counterpart tests: SB-CL-06 versus SB-DVI-09. The same initial and boundary conditions were used except for different locations of the cold leg and DVI nozzle, respectively. A comparison of the maximum PCT behavior is shown in Figure 17. It was found that the maximum heater surface temperature increased more in the SB-DVI-09 test than in the SB-CL-06 test, indicating that the DVI line break is more limiting than the corresponding cold leg break. As the DVI nozzle is located at a higher elevation than the cold leg, a higher core pressure is required to overcome the hydraulic static head in the downcomer region between the cold leg and DVI nozzle. This results in a lower and delayed core water level than the cold leg break case as shown in Figure 18 [20].

An inadvertent opening of the POSRV test was carried out as one of the SBLOCA spectra to construct a validation database for the Safety and Performance Analysis Computer Code (SPACE), which is under development. A break at a POSRV installed at the top head of the pressurizer was taken into account. Due to its small break size, the other phases except for the blow-down phase were not observed in the test. The loop seal was not cleared during the test period and the SITs were not activated. Measured primary and the secondary pressure trends are shown in Figure 19.

The coolant in the RCS remained in the liquid phase throughout most of the blow-down period, but steam began to form in the upper head, upper plenum, and hot legs as the blow-down period came to an end. The rapid depressurization ended when the pressure decreased to just above the saturation pressure of the SG secondary side. The break flow was in a single-phase liquid condition throughout the blow-down period [21].

A counterpart test to the SB-CL-18 of the LSTF was carried out to evaluate the scale-up capability of ATLAS. SB-CL-18 was a 5% cold break test and was utilized as ISP-26 under OECD/NEA WGAMA activity [22]. The integral (or global) scaling ratios of ATLAS with respect to the LSTF were calculated to be 1/1.84 in height, 1/1.59 in diameter, 1/4.65 in volume, and 1/3.45 in flow rate. The length scaling ratio can be different depending on which reference length is used in this global scaling. Here, the active core length was used as a reference height scaling. In order to determine the appropriate boundary conditions for simulating SB-CL-18 with ATLAS, the boundary flow scaling methodology was used to preserve the mass and energy as follows [23]:

$$\left(\frac{\tau m_{\text{out}}}{M_o}\right)_R = 1, \qquad \left(\frac{\tau m_{\text{in}}}{M_o}\right)_R = 1, \qquad \left(\frac{\tau Q}{M_o h_c}\right)_R = 1. \tag{3}$$

From (3), the break flow can be scaled

$$m_{\text{out,R}} = \frac{M_{o,R}}{\tau_R} = \frac{m_{\text{out,ATLAS}}}{m_{\text{out,LSTF}}} = \frac{{D_{\text{out,ATLAS}}}^2}{{D_{\text{out,LSTF}}}^2}, \tag{4}$$

where

$$M_{o,R} = \frac{M_{\text{ATLAS}}}{M_{\text{LSTF}}} = \frac{1.63}{7.23} = 0.22545, \qquad \tau_R = \frac{\tau_{\text{ATLAS}}}{\tau_{\text{LSTF}}} = \frac{1}{\sqrt{2}}. \tag{5}$$

Thus, the break diameter can be calculated from (4) as follows:

$$D_{\text{out,ATLAS}} = D_{\text{out,LSTF}}\sqrt{\frac{M_{o,R}}{\tau_R}} = 22.5\sqrt{0.3188} = 12.7\,\text{mm}. \tag{6}$$

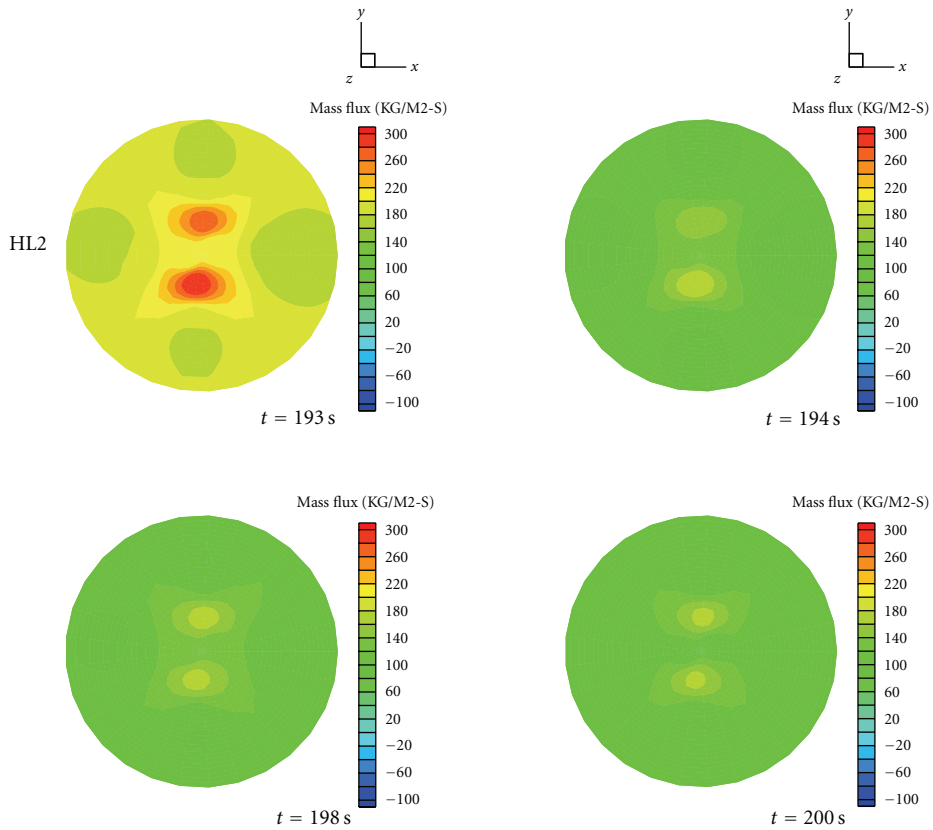

Figure 15: MARS-3D prediction of total mass flux at 11th elevation in the core, $z = 1645$ mm (SB-DVI-09).

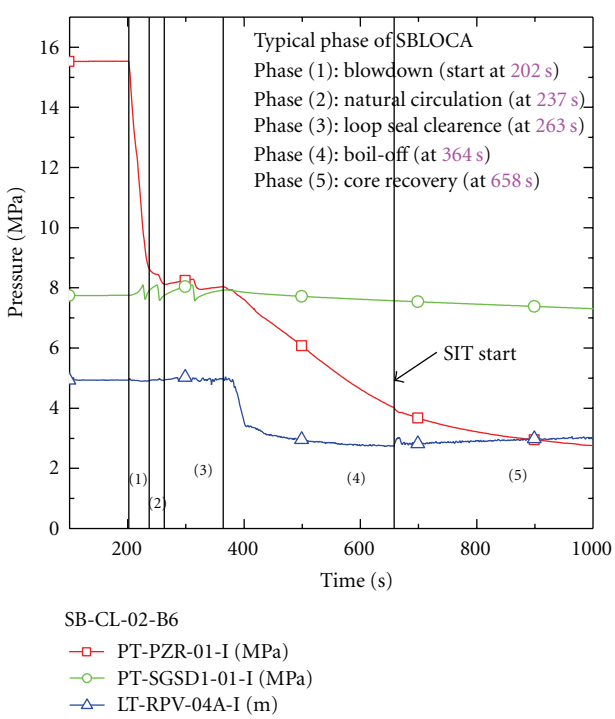

Figure 16: Identification of characteristic phases during the present SBLOCA test period.

Similar to the break nozzle, the safety injection flow rate and core power were scaled as follows:

$$m_{\text{in,ATLAS}} = \frac{M_{o,R}}{\tau_R} \cdot m_{\text{in,LSTF}} = 0.3188 \cdot m_{\text{in,LSTF}}, \quad (7)$$

$$Q_{\text{ATLAS}} = \frac{M_{o,R}}{\tau_R} \cdot Q_{\text{LSTF}} = 0.3188 \cdot Q_{\text{LSTF}}. \quad (8)$$

However, a smaller core power than an LSTF was applied to ATLAS because of its electrical power limit, as shown in Figure 20.

A comparison of the measured primary pressure with the LSTF measurement is shown in Figure 21. A delayed loop seal clearing occurred in the ATLAS test, and a steeper decrease in the primary pressure occurred after the loop seal clearing was obtained. Measured differential pressure and water levels are shown in Figure 22. In the LSTF test, a significant and rapid water level depression was observed, whereas in the ATLAS test, a relatively smooth water level depression was obtained. These differences seem to be caused by differences in loop configurations, elevation distributions of the major components, and core power between two facilities. Nonetheless, this counterpart test showed a promising prospect of the scale-up capability of ATLAS, and a more rigorous analysis is underway.

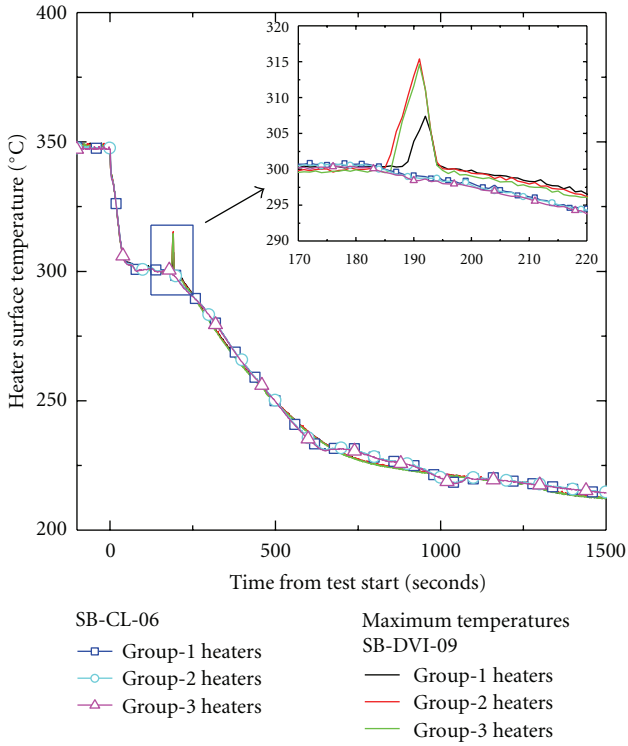

Figure 17: Comparison of cladding temperatures between SB-DVI-09 and SB-CL-06.

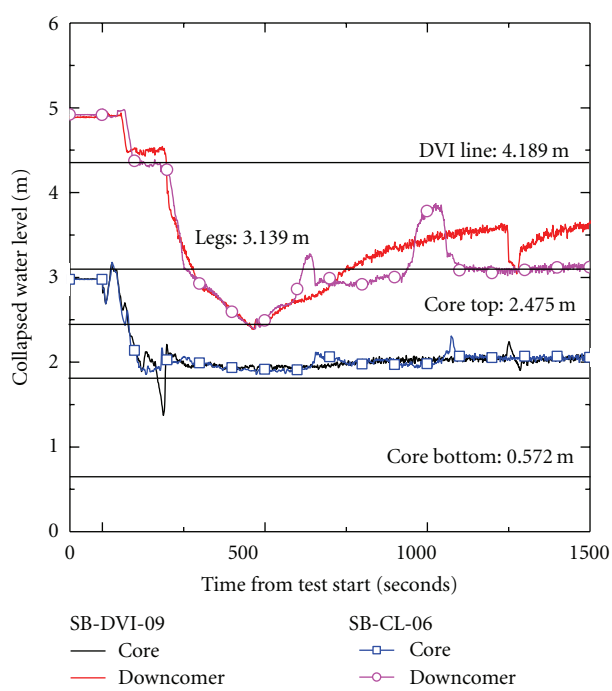

Figure 18: Comparison of the water levels between SB-DVI-09 and SB-CL-06.

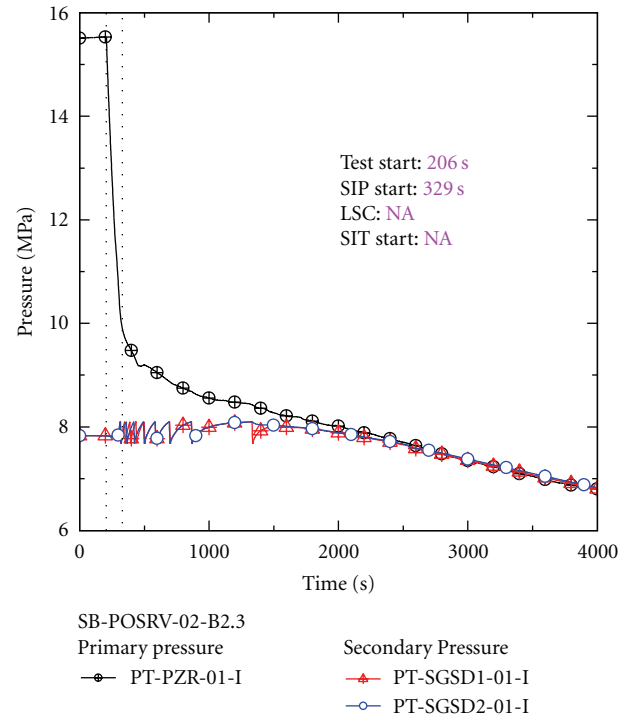

Figure 19: Primary and secondary pressure behavior during SB-POSRV-02-B2.3.

4.4. Steam Generator Tube Rupture (SGTR) Tests. An SGTR accident is a penetration of the barrier between the RCS and secondary system and is one of the design basis accidents having a significant impact on safety from the viewpoint of radiological release. This accident has a relatively higher occurring frequency, and the estimated frequency of a single SGTR is 1.5×10^{-2} per reactor year (RY) [24].

In order to simulate the SGTR accident of the APR1400, several tests, defined in Table 5, were performed by simulating a double-ended rupture of either a single or five U-tubes at either the hot or cold side of the ATLAS steam generator. Regarding a multiple steam generator tube rupture (MSGTR), there is demand for a design mitigating the MSGTR consequences for up to five U-tube ruptures, and on lowering the containment bypass to improve the design and operational procedures. The NRC estimated frequency for a multiple SGTR event is approximately 8.4×10^{-4}/RY [24].

A break was simulated using an external break simulating pipe, and its diameter was increased by a factor of $\sqrt{2}$ in order to simulate the double-ended guillotine break as shown in Figure 23. Different break locations—SG inlet plenum and outlet plenum—were simulated to see the effects of the break locations. A boundary flow scaling approach was taken to simulate a scaled break flow rate in the test. During the SGTR, the break flow can be choked or not depending on the differential pressure between the primary and secondary systems. A break spool piece, which consisted of an orifice and a tube, was designed to simulate both the choking or nonchoking break flow. Five U-tube ruptures were simulated in five tubes connected in parallel, as shown in Figure 24.

Table 5: Test matrix for SGTR tests.

Test ID	APR1400 Number of broken U-tubes/break area (inch)	Break location	Type of Rx. trip
SGTR-HL-04	1 ea/0.67	2 m hot side	HSGL*
SGTR-HL-05	5 ea/3.35	2 m hot side	HSGL
SGTR-HL-06	1 ea/0.67	2 m hot side	LPP**
SGTR-HL-07	5 ea/3.35	2 m hot side	LPP
SGTR-CL-01	1 ea/0.67	2 m cold side	HSGL
SGTR-CL-02	5 ea/3.35	2 m cold side	HSGL

*HSGL: High Steam Generator Level.
**LPP: Low Pressurizer Pressure.

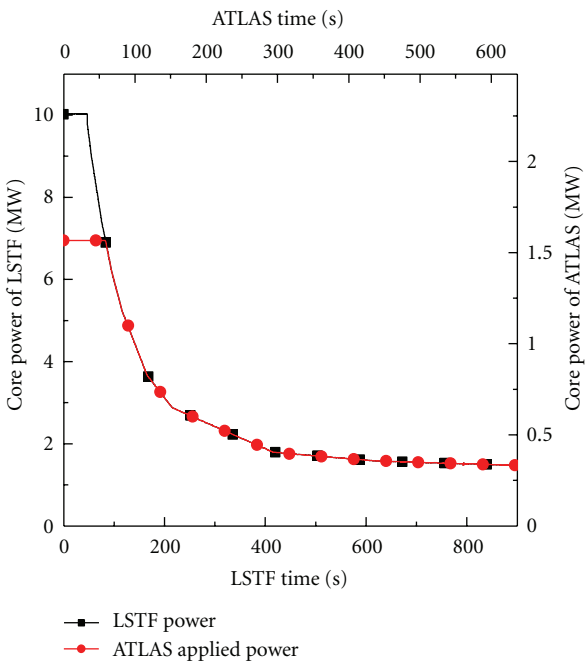

Figure 20: Comparison of the applied power in the LSTF counterpart test.

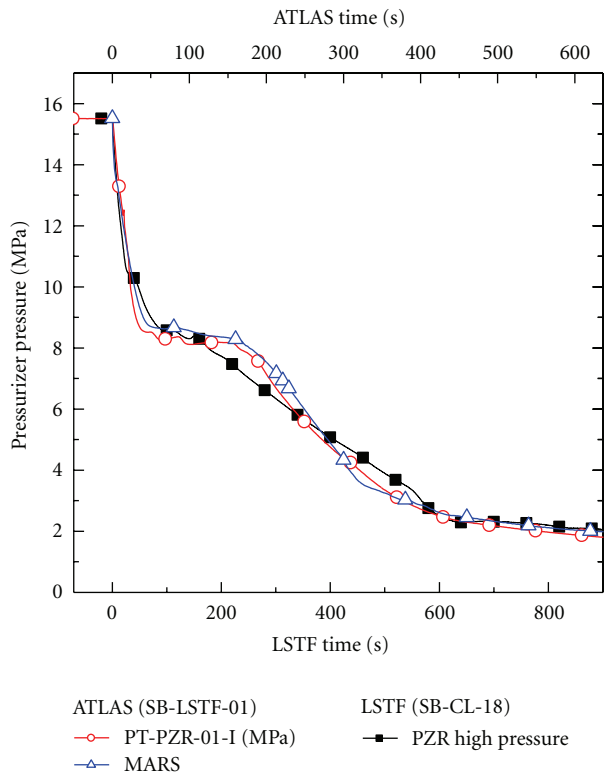

Figure 21: Comparison of the primary pressure in the LSTF counterpart test.

Two types of reactor trip conditions were used: HSGL and LPP.

A typical measured primary pressure for a single U-tube rupture is shown in Figure 25. In this figure, AFAS stands for Auxiliary Feedwater Actuation Signal and it implies that auxiliary feedwater was provided into the intact steam generator between 3153 s and 3911 s. More information can be found in the literature [25]. The typical sequence of events was experimentally identified. It was found that the break location affected the leak flow rate. The break at the cold side, where the external break simulating pipe was connected to the outlet plenum of the SG, resulted in a higher leak flow rate than the break at the hot side. However, the effect was not as significant as at the break area. In the case of the five U-tube ruptures, the safety injection pump was actuated earlier than in the single U-tube rupture due to higher depressurization. Earlier injection of cold ECC water reduced the average fluid temperature of the RCS, resulting in less heat transfer to the secondary side. Thus, the secondary pressure increased more slowly than in the single U-tube rupture case, eventually causing a retardation of the MSSV opening.

4.5. Feed Line Break (FLB) Tests. After the major tests on LOCA were completed, feed water line breaks were investigated as one a typical non-LOCA design basis accident. The effects of the break locations and break sizes were experimentally examined. The APR1400 has two nozzles for a feedwater supply: an economizer and a downcomer nozzle. Under normal operating conditions, 90% feedwater is supplied through the economizer, and the remaining 10% is provided through the downcomer nozzle for high thermal efficiency. Thus, two different nozzles were assumed to be broken in the

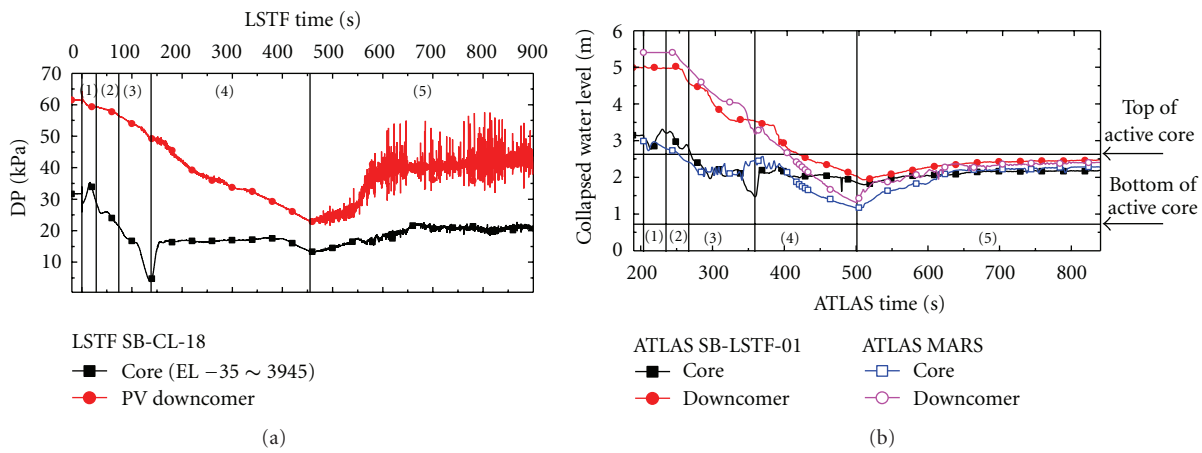

Figure 22: Comparison of collapsed water levels in the LSTF counterpart test.

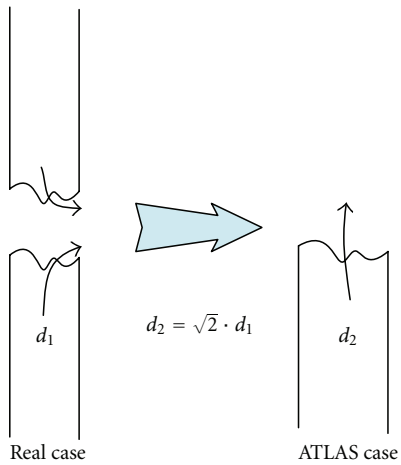

Figure 23: Simulation concept of the guillotine break of a SG U-tube.

Table 6: Test matrix for FLB tests.

Test ID	Break size APR1400 (area: ft^2)	Break size ATLAS (mm)	Break location	Type of Rx. trip
FLB-EC-01	0.4	15.24	Economizer	HPP*
FLB-EC-02	0.1	7.62	Economizer	HPP
FLB-EC-03	0.86	22.29	Economizer	HPP
FLB-EC-04	0.4	15.24	Economizer	LSGP**
FLB-DC-01	0.18	10.23	Downcomer	HPP

* HPP: High Pressurizer Pressure.
** LSGP: Low Steam Generator Pressure.

ATLAS test. According to the safety analysis results, the break of the economizer nozzle is found to be more limiting from the viewpoint of the pressurization of the primary system. However, the break of the downcomer nozzle is more or less close to a steam line break accident. Several different break sizes from 0.1 ft^2 (0.0093 m^2) to 0.86 ft^2 (0.0799 m^2) were taken into account. A test matrix is shown in Table 6.

Typical pressure trends at the pressurizer and steam generator dome are shown in Figure 26. Upon the break, the affected steam generator was rapidly depressurized. As ATLAS has a maximum power of 10%, pressurization of the primary system after the FLB could not be simulated realistically. Thus, the high pressurizer pressure trip (HPP) was intentionally triggered 10.6 seconds after the break. Contrary to the affected steam generator, the intact steam generator was pressurized until opening the MSSVs. This integral effect test data is being used to evaluate the prediction capability of the safety analysis codes, such as the MARS, RELAP5, and SPACE codes.

4.6. Steam Line Break (SLB) Tests. Compared with the feed line breaks, the main steam-line break in a pressurized water reactor is a core overcooling event characterized by a strong positive moderator reactivity feedback that can ultimately overcome the core shutdown margin. One of the most important safety concerns of SLB accidents is the return to power. The key thermal-hydraulic phenomena for the SLB transient include a fluid flashing in the reactor upper head and hot legs, a forced and natural circulation flow in the primary system, a steam generator heat transfer, and an asymmetric temperature distribution in the lower plenum of the core.

A similarity analysis of the ATLAS facility with an SLB event was analyzed, and it was confirmed that ATLAS has a reasonable similarity with respect to the prototype plant [26, 27].

A series of integral effect tests simulating various transient conditions were performed. The loss of offsite power (LOOP) was considered as one of the parameters to determine a test matrix for SLBs. The effects of the break area were also considered, based on the flow restrictor geometry at the exit nozzle of the steam generator. A test matrix for the SLB tests is shown in Table 7.

Measured pressure trends are shown in Figure 27. Upon a break, the primary pressure was rapidly depressurized and was recovered by actuation of the safety injection pump at around 500 seconds. The affected steam generator was rapidly depressurized, and the water inventory was also depleted within a short period of time. Though auxiliary feed

Table 7: Test matrix for SLB tests.

Test ID	Break size	Test conditions
SLB-GB-01	Guillotine break	100% rated condition with LOOP
SLB-GB-02	Guillotine break	8% power condition without LOOP
SLB-GB-03	Guillotine break	8% power condition with LOOP
SLB-PB-01	20% partial beak	100% rated condition with LOOP
SLB-PB-02	20% partial beak	8% power condition without LOOP
SLB-PB-03	20% partial beak	8% power condition with LOOP

* LOOP: Loss of Offsite Power.

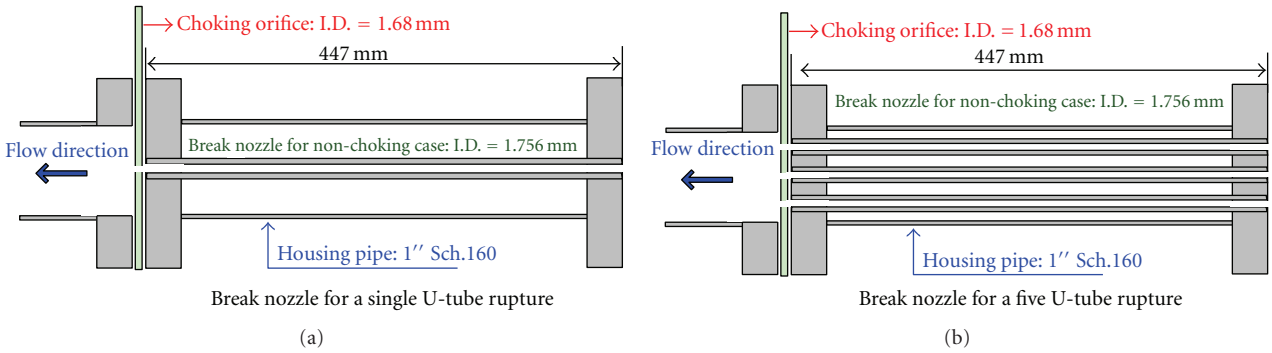

Figure 24: Designed break nozzles for a SGTR and MSGTR.

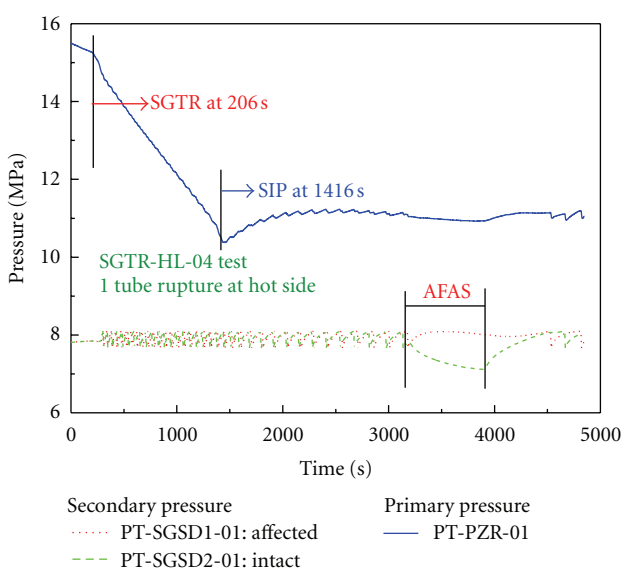

Figure 25: Typical trend of the primary pressure during the SGTR-HL-04 test.

water was provided to the broken steam generator, the water level was not recovered due to a large break size. The intact steam generator was also depressurized initially, but it was isolated when the low steam generator pressure (LSGP) trip signal was activated. Strong loop asymmetric behavior was observed and major thermal-hydraulic information was obtained.

5. Future Prospect

Nuclear power plants featuring more advanced safety and economic competitiveness than the current commercial nuclear plants in operation are essential in the world nuclear market. In particular, safety was a prime importance before the Fukushima accident, too. The Fukushima accident attracted national attention to high-risk multiple failures. In particular, an event that has an extremely low occurring frequency but results in high core damage frequency if it occurs needs to be reconsidered from the viewpoint of the "defense in depth" concept. Accidents not seriously considered from a design basis such as a station blackout (SBO), an anticipated transient without scram (ATWS), reactor vessel rupture (RVR), total loss of feed water (TLOFW), and medium break LOCA are considered as high-risk multiple failure accidents as safety concerns regarding severe accidents have magnified after the Fukushima accident.

Many people have become recently concerned about the safety of operating nuclear power plants in connection with the SBO accident. Therefore, SBO-related integral effect tests have the first priority in the coming ATLAS program. The SBO accident itself and multiple SBO-induced accidents, for instance, an SBO combined with LOCA, will be investigated in the near future. Primary inventory loss due to either opening the POSRV or leakage of the RCP seal can be one of the promising candidates. In addition, new safety features to mitigate the SBO accident efficiently are being proposed, and such concepts can be validated by performing a simulation with the ATLAS facility.

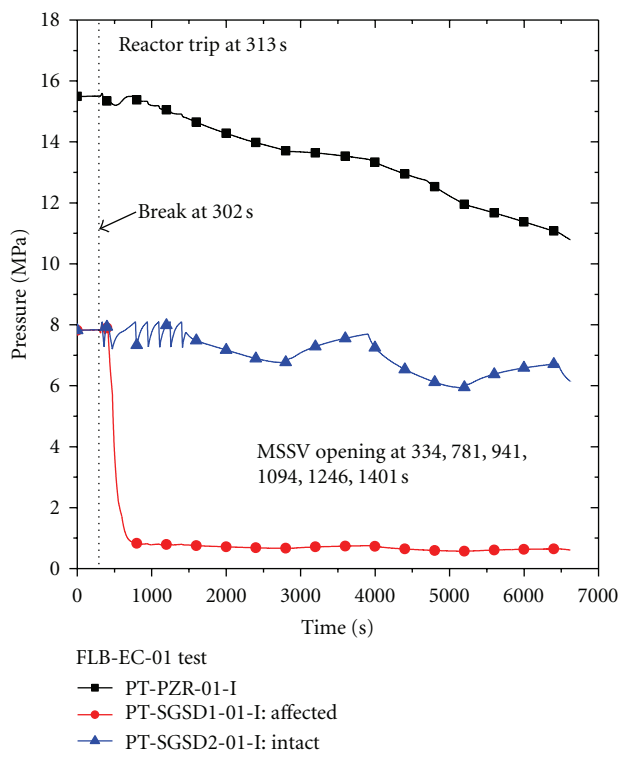

Figure 26: Pressure trends at the pressurizer and steam generator dome.

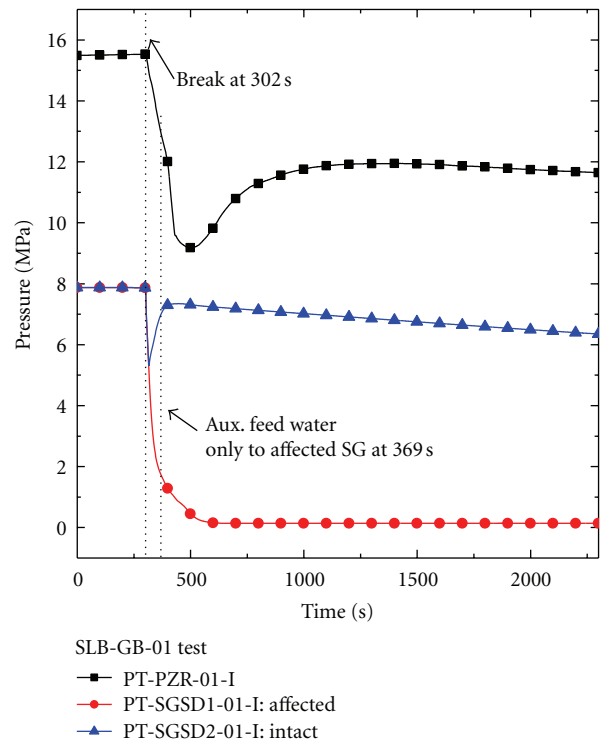

Figure 27: Pressure trends of the guillotine break of the steam line.

The NRC is planning to make risk-informed changes to 10CFR50.46 (ECCS acceptance criteria). As Korean regulations are primarily based on the NRC's regulations, the NRC's changes in regulatory position will significantly affect the domestic regulatory environment. In particular, a redefinition of a design-basis LOCA accident is a safety issue from the viewpoint of safety enhancement. The present domestic regulatory R&D is focusing on the safety analysis methodology of a LOCA larger than the transition break size (TBS) LOCA. Thus, the TBS LOCA of domestic plants needs to be analyzed, and the safety against a TBS LOCA should be validated. An integral effect test program focusing on a TBS LOCA is being planned. The Korean industry is developing a specific advanced nuclear power plant, called an advanced power reactor plus (APR+) to enhance safety and reliability by adopting advanced technology such as a passive feature [28, 29]. Among the newly introduced safety features, the passive auxiliary feedwater system (PAFS) completely replacing the existing active auxiliary feedwater system highlights the advanced technology. An integral effect test program to validate the heat removal performance of the PAFS has already been launched. In the first phase, one steam generator of ATLAS will be connected to the PAFS, and integral effect tests including a performance test will be performed in early 2012. Natural circulation characteristics along the PAFS loop, condensation performance inside the heat exchanger tube, pool boiling, and mixing phenomena in the large passive condensate cooling tank (PCCT) will be investigated in order to support its licensing process within its due schedule.

Even though the LBLOCA reflood tests were already completed in 2007, further expanded tests are on demand by domestic industry according to change in number of electrical trains of the ECCS in the APR1400. When the number of electrical trains is increased from 2 to 4, the safety injection water is introduced through three DVI nozzles rather than two nozzles. At the moment, the APR1400 is under a pre-application review process of the US NRC to get a design approval. Therefore, further supporting activities are waiting for the ATLAS.

Nowadays, only a few integral effect test facilities are available and a few are under refurbishment in the world. As the facilities available now or soon are based on their specific prototype plants, they cannot be a universal provider of the integral effect data. That is the main reason why many counterpart tests were performed in the past. Therefore, the ATLAS can be utilized together with other facilities to effectively solve the safety issues and interests as a future prospective.

6. Summary and Conclusions

ATLAS is a large integral effect test facility scaled down from the APR1400 at 1/2 in height and 1/288 in volume. This is considered by the international community as one of critical facilities to be monitored in the long term in the field of thermal hydraulics of an ALWR [30]. Since its first operation at the end of 2006, an integral effect database was established for major design-basis accidents of the APR1400, including LBLOCA reflood, SBLOCA, SGTR, FLB, and SLB tests.

The LBLOCA reflood test data were of critical importance to support a domestic licensing process of the APR1400. Technically, the ECC bypass and downcomer boiling issues were considered seriously to understand their physical phenomena and to assess the predictability of the safety analysis codes. In the SBLOCA tests, both a DVI line and cold leg break were simulated, and the phenomenological difference was investigated. It was experimentally confirmed that the DVI line break is a more limiting accident than the equivalent size break at the cold leg. Several sensitivity tests were accomplished in the SGTR tests. In addition to a single SGTR, a multiple SGTR of five U-tube ruptures was simulated. The effects of break location were also experimentally investigated.

Two major non-LOCA design-basis accidents such as the FLB and SLB were continued after completion of the above-mentioned LOCA series tests. These databases are being used to reduce the design uncertainties and validate the models and correlation of the safety analysis codes under improvement or development.

During past short operating experiences, the operational technique and managing system of the ATLAS facility were set up well. In particular, successful coordination of the ISP-50 and domestic cooperation programs enabled the ATLAS data to be trusted within the relevant thermal-hydraulic communities.

Demands on the integral effect tests with ATLAS are increasing mainly due to the active nuclear R&D program in Korea. Either design modifications or new design concepts introduced to new plants in order to improve their safety and economic efficiency will be validated through the ATLAS test in the near future. In particular, after the Fukushima accident, much attention was placed on the safety of the existing plants. Thus, further experimental needs are expected to increase.

Finally, as public interest is being focused on beyond design basis accidents (BDBAs) due to the Fukushima accident, integral effect test facilities should be utilized to produce clearer knowledge of the actual phenomena and to provide the best guideline for accident management.

Acknowledgments

This work was carried out under the support of Ministry of Education, Science, and Technology (MEST) of the Korean government, under the national nuclear mid- and long-term R&D program.

References

[1] W. P. Baek, C. H. Song, B. J. Yun, T. S. Kwon, S. K. Moon, and S. J. Lee, "KAERI integral effect test program and the ATLAS design," *Nuclear Technology*, vol. 152, no. 2, pp. 183–195, 2005.

[2] Y. S. Kim, K. Y. Choi, H. S. Park et al., "Commissioning of the ATLAS thermal-hydraulic integral test facility," *Annals of Nuclear Energy*, vol. 35, no. 10, pp. 1791–1799, 2008.

[3] W. P. Baek, Y. S. Kim, and K. Y. Choi, "LBLOCA and DVI line break tests with the ATLAS integral facility," *Nuclear Engineering and Technology*, vol. 41, no. 6, pp. 775–784, 2009.

[4] K. Y. Choi et al., "Effects of break size on DVI Line break accidents of the ATLAS," *Nuclear Technology*, vol. 175, pp. 604–618, 2011.

[5] EPRI, "EPRI Utility Requirement Documents for the Advanced Light Water Reactor (Chapter 5)," 1995.

[6] K. Y. Choi et al., "OECD/NEA/CSNI International Standard Problem No. 50: Final Integration Report Volume I, II, III, Analysis of Blind/Open Calculations," NEA/CSNI/R(2012)6.

[7] M. Ishii, S. T. Revankar, T. Leonardi et al., "The three-level scaling approach with application to the Purdue University Multi-Dimensional Integral Test Assembly (PUMA)," *Nuclear Engineering and Design*, vol. 186, no. 1-2, pp. 177–211, 1998.

[8] W. P. Baek et al., "Thermal hydraulic integral effect tests for advanced reactors (in Korean)," KAERI/RR-2240/2001, 2002.

[9] N. Aksan, "International standard problems and small break loss-of-coolant accidents (SBLOCA)," *Science and Technology of Nuclear Installations*, vol. 2008, Article ID 814572, 22 pages, 2008.

[10] MPR-1324, "Summary of results from the UPTF downcomer injection/vent valve separate effects tests: Comparison to previous scaled tests, and application to Babcock&Wilcox pressurized water reactors," 1992.

[11] H. S. Park, K. Y. Choi, S. Cho et al., "Major findings from LBLOCA reflood tests using the ATLAS facility," *Nuclear Engineering and Design*, vol. 240, no. 12, pp. 3920–3929, 2010.

[12] H. S. Park, K. Y. Choi, S. Cho, K. H. Kang, Y. S. Kim, and W. P. Baek, "An integral effect test on the LBLOCA reflood phenomena for the APR1400 using ATLAS under a best-estimate condition," *Journal of Nuclear Science and Technology*, vol. 46, no. 11, pp. 1059–1069, 2009.

[13] H. S. Park, K. Y. Choi, S. Cho et al., "An integral effect test on the reflood period of a large-break LOCA for the APR1400 using ATLAS," *Nuclear Technology*, vol. 170, no. 1, pp. 100–113, 2010.

[14] H. S. Park, K. Y. Choi, S. Cho, K. H. Kang, and Y. S. Kim, "Major thermal-hydraulic phenomena found during ATLAS LBLOCA reflood tests for an advanced pressurized water reactor APR1400," *Nuclear Engineering and Technology*, vol. 43, no. 3, pp. 257–270, 2011.

[15] H. S. Park, J. H. Jeong, K. Y. Choi et al., "A separate effect test on the cooling behavior in a pressurized water reactor core under a low reflooding rate condition by using ATLAS and RELAP5/MOD3.3 code assessment," *Annals of Nuclear Energy*, vol. 38, no. 5, pp. 1053–1064, 2011.

[16] J. J. Jeong, K. S. Ha, B. D. Chung, and W. J. Lee, "Development of a multi-dimensional thermal-hydraulic system code, MARS 1.3.1," *Annals of Nuclear Energy*, vol. 26, no. 18, pp. 1611–1642, 1999.

[17] K. Y. Choi, H. S. Park, S. Cho et al., "Experimental Simulation of a Direct Vessel Injection line break of the APR1400 with the ATLAS," *Nuclear Engineering and Technology*, vol. 41, no. 5, pp. 655–676, 2009.

[18] Mitsubishi heavy industries, Ltd, "Small break LOCA sensitivity analyses for US-APWR," MUAP-07025-NP(R0), 2007.

[19] S. Cho, K. Y. Choi, H. S. Park et al., "Integral effect experiments on 6 inch cold-leg SBLOCA using the ATLAS facility," in *International Congress on Advances in Nuclear Power Plants (ICAPP '10)*, pp. 1375–1384, June 2010.

[20] H. S. Park, K. Y. Choi, S. Cho, K. H. Kang, and Y. S. Kim, "Counterpart tests of SBLOCA on the effect of break location with the ATLAS: DVI nozzle versus cold-leg breaks," *Journal of Nuclear Science and Technology*, vol. 48, no. 10, pp. 1319–1326, 2011.

[21] S. Cho et al., "Integral effect test for an inadvertent opening of POSRV using the ATLAS facility," in *18th International Conference on Nuclear Engineering (ICONE '10)*, Xian, China, May 2010.

[22] Y. Kukita et al., "ISP-26, OECD/NEA/CSNI International Standard Problem No.26, ROSA-IV LSTF cold-leg small-break LOCA experiment, Comparison report," OECD/NEA/ CSNI/ R(91)13, 1992.

[23] S. Cho et al., "Counter-part test results of the LSTF SB-CL-18 using the ATLAS," in *Korean Nuclear Society Autumn Meeting*, Jeju, Korea, October 2010.

[24] J. Taylor, "Policy, technical, and licensing issues pertaining to evolutionary and advanced light-water reactor (ALWR) design," SECY-93-087, NRC, 1993.

[25] K. H. Kang et al., "Integral effect test on the transient thermal-hydraulic behavior during the steam generator tube rupture accident in the APR1400," to appear in *Nuclear Technology*.

[26] K. Y. Choi, H. S. Park, D. J. Euh, T. S. Kwon, and W. P. Baek, "Simulation capability of the ATLAS facility for major design-basis accidents," *Nuclear Technology*, vol. 156, no. 3, pp. 256–269, 2006.

[27] K. Y. Choi et al., "Thermal hydraulic similarity analysis of the integral effect test facility for main steam line break events," in *the 11th International Topical Meeting on Nuclear Reactor Thermal-Hydraulics (NURETH '05)*, Avignon, France, October 2005.

[28] C. H. Song et al., "Thermal-hydraulic R&Ds for the APR+ developments in Korea," in *Proceedings of the 18th International Conference on Nuclear Engineering (ICONE '10)*, Xian, China, May 2010.

[29] C. H. Song et al., "Advanced design features and the thermal-hydraulic tests for the APR+ reactor," in *Proceedings of the 2011 International Congress on Advances in Nuclear Power Plants (ICAPP '11)*, Nice, France, May 2011.

[30] "Nuclear safety research in OECD countries, support facilities for existing and advanced reactors (SFEAR)," NEA/CSNI/ R(2007)6, 2007.